ELSEVIER

Journal of Nuclear Materials 275 (1999) 63–73

journal of nuclear materials

www.elsevier.nl/locate/jnucmat

Determination of displacement threshold energies in pure Ti and in γ-TiAl alloys by electron irradiation

G. Sattonnay [a], F. Rullier-Albenque [b], O. Dimitrov [a,*]

[a] *CECM-CNRS, 15 rue Georges Urbain, F94407 Vitry-Sur-Seine cedex, France*
[b] *LSI-CEA-Ecole Polytechnique, F91128 Palaiseau, France*

Received 23 December 1998; accepted 26 March 1999

Abstract

Resistivity damage rates, determined during low-temperature electron irradiations in the energy range 0.3–2.5 MeV, were used for evaluating displacement threshold energies of titanium in high purity hcp titanium, and of titanium and aluminium in γ-TiAl intermetallic compounds. These parameters were deduced from a comparison of experimental displacement cross-section variations as a function of electron energy, with theoretical curves based on a displacement model for diatomic materials. The displacement energy of titanium in hcp titanium appears to depend on the electron energy. A threshold value of 21 ± 1 eV was obtained in the range 0.3–0.5 MeV, and a larger value of 30 ± 2 eV is determined in the range 0.5–2.5 MeV. In γ-TiAl, aluminium atoms are displaced first, with a threshold displacement energy (34 ± 2 eV) larger than the one of titanium atoms, and much higher than the value in pure aluminium. The displacement energy of Ti atoms is 28 ± 2 eV, close to the one obtained in pure titanium under similar conditions. These results were used for re-evaluating the Frenkel-pair resistivity of the stoichiometric TiAl compound.

1. Introduction

In pure metals, radiation damage production has been extensively studied as a function of the energy of incident particles, and atomic displacement threshold energies have been determined for many elements. By contrast, alloys and intermetallic compounds have been much less investigated, although radiation damage effects in these materials are of both fundamental and technological importance.

TiAl-based intermetallic compounds are attractive candidates for high-temperature applications in the aerospace and automobile industries. In addition, TiAl compounds have recently been considered as potential nuclear materials [1], due to their high creep resistance and to their low neutron-induced radioactivity as compared to those of austenitic stainless steels [2]. Although TiAl-based materials have very limited room-temperature deformation capacity, this does not necessarily preclude the planned nuclear applications, since these involve static parts operating in a temperature range (around 800°C) where the material displays significant ductility. Also, the growth rate of defect clusters under electron or neutron irradiation is limited, and a high swelling resistance was observed [3,4].

Atomic displacement data have been previously obtained in long-range ordered (LRO) Ni_3Al intermetallics and in Ni(Al) solid solutions [5], in LRO and disordered CuAu and Cu_3Au compounds [6,7] and in tantalum carbides [8,9] by analyzing the resistivity damage rates during electron irradiations. In the superconducting compounds Nb_3Ge and V_3Si, combined determinations of the decrease in critical temperature and of the resistivity increase have provided selective evidence for the displacement of each atomic species, and allowed the respective threshold energies to be evaluated [10]. Up to now, the effects of irradiation on γ-TiAl have been little investigated and no experimental values of the threshold displacement energy E_d are available in titanium aluminides. Concerning defect production during irradiation, some results were obtained by electrical resistivity measurements on γ-TiAl electron irradiated at 21 K [11].

* Corresponding author. Tel.: +33-1 46 87 35 93; fax: +33-1 46 75 04 33; e-mail: dimitrov@glvt-cnrs.fr

0022-3115/99/$ – see front matter
PII: S0022-3115(99)00109-9

Evaluations of the Frenkel-pair resistivity and of the disordering contribution to the resistivity damage rate were obtained. The mobilities of irradiation-induced defects have been determined by investigating the recovery after electron irradiation by electrical resistivity measurements [11] or by positron lifetime spectroscopy [12–14], or after proton irradiation by positron lifetime measurements [12]. From these experiments, it appears that radiation-induced interstitials become mobile around 80 K and that vacancies migrate at ~440 K in the stoichiometric TiAl compound [11,14]. Computer simulations of the displacement processes in several directions in γ-TiAl have been performed by Wang et al. [15], using molecular dynamics with N-body potentials. The authors found that ⟨1 1 0⟩ rows containing only Al (or Ti) atoms, were the easiest directions for defect production and the threshold energies to produce a Frenkel-pair in these directions were less than 20 eV. In this case, their model predicts, after a replacement collision sequence along the ⟨1 1 0⟩ direction, that the resulting Frenkel-pair consists of a vacancy on the Al (or Ti) sublattice and an Al (or Ti) interstitial with crowdion configuration on a [1 1 0] row formed only by Al (or Ti) atoms, rather than a vacancy and a dumbbell interstitial.

In the present work, we have examined by electrical resistivity measurements the damage production at low temperature (21 K) in $L1_0$ LRO γ-TiAl, irradiated by electrons in the energy range from 0.3 to 2.5 MeV. The effective threshold energies E_d^{Ti} and E_d^{Al} for each atomic species were obtained by a comparison of the energy dependence of the displacement cross-sections, resulting from the analysis of the experimental resistivity damage rates, with theoretical curves calculated for different values of E_d^{Ti} and E_d^{Al} (from [24]).

Together with the investigated TiAl compounds, a high purity titanium sample was also irradiated. A small number of experiments have been reported on near-threshold irradiation of pure titanium [16,17,25], and the results may be influenced by the relatively high concentration of impurities usually present in the metal. In the present work, we used high purity titanium with a very low oxygen content, both for the elaboration of the TiAl compounds and as a reference material during irradiation. Due to the availability of this high-purity material, and as a validation of the experimental procedure, the determination of the effective displacement threshold energy was also performed in the pure titanium irradiated in the same experiments as the TiAl alloys.

2. Experimental procedure

The investigated materials were binary TiAl compounds with nominal concentrations of 50 and 53 at.% Al. They were prepared from high-purity metals by RF levitation melting followed by directional solidification and homogenized by annealing for 24 h at 1400 K, as described in Ref. [18].

The investigated pure titanium had a very low oxygen concentration (30 wt ppm) and the main impurities were carbon (60 wt ppm) and tungsten (46 wt ppm). The final composition of the alloys was checked by inductively coupled plasma atomic emission spectroscopy (ICP-AES). Some deviations from the nominal compositions were detected, and the actual compositions were evaluated based on the $R_{4.2\,K}/R_{294\,K}$ electrical resistance ratios [19]: the Al concentrations were, respectively, 50.1 and 52.5 (Table 1). To check the contamination by impurities possibly introduced during the elaboration process, the oxygen content was measured by activation analysis in the homogenized alloys. The final oxygen content was found to be around 75 wt ppm (as compared to ~30 wt ppm existing initially in titanium). Therefore, some oxygen was introduced in our alloys, but its concentration remains very low comparatively to the one usually observed in this type of compounds (at least 300 wt ppm). X-ray diffraction and transmission electron microscopy showed that the alloys had a single-phase $L1_0$ structure.

The Ti samples were spark-cut from cold rolled ~25 μm thick foils. TiAl specimens were prepared by diamond sawing and mechanical polishing, as described in Ref. [11], then further thinned to 60 μm by chemical polishing with a solution 10 vol.% HF, 30 vol.% H_2O_2 and 60 vol.% H_2O. The samples were annealed in a vacuum of 10^{-6} Pa for 10 h at 743 K (Ti) or 1223 K (TiAl), then furnace cooled.

The irradiation experiments were performed in the liquid hydrogen cryostat of the Van de Graaff electron accelerator at the LSI, Ecole Polytechnique, Palaiseau (France). The samples were maintained at 21 K in the liquid hydrogen bath, separated from the accelerator vacuum by a 25 μm thick steel window. The radiation damage produced by electrons of constant energy was investigated by determining the electrical resistivity variations as a function of fluence. The resistivity measurements were performed at 21 K using standard four-point DC measurements. The shape factors of the TiAl samples, $k = \rho_{4.2\,K}/R_{4.2\,K}$, were deduced from their 4.2 K electrical resistances before irradiation using resistivity values determined on separate specimens of suitable shape (~1 mm^2 in cross-section), annealed in the same conditions as above. The shape factor of the titanium

Table 1
Composition of materials, 4.2 K electrical resistivities (ρ_0) of unirradiated samples and experimental resistivity damage rates ($\Delta\rho/\Delta\phi$) determined during irradiation with 1.4 MeV electrons

	Ti	$Ti_{50}Al_{50}$	$Ti_{47}Al_{53}$
Al-content (at.% Al)	–	50.1	52.5
ρ_0 (μΩ cm)	0.496	5.58	39.59
$\Delta\rho/\Delta\phi$ (10^{-25} Ω cm^3)	1.34	1.56	1.16

sample was calculated from the titanium ideal resistivity at 294 K ($\rho_i = 46.40$ μΩ cm, determined from [20]), by using the relationship $k = \rho_i/(R_{294\,K} - R_{4.2\,K})$. The uncertainty on resistivity variations was 1×10^{-9} Ω cm. The residual resistivity values of the pure titanium and of the TiAl alloys are reported in Table 1.

During irradiation, the electron flux i_b was measured on a Faraday cup permanently placed behind the samples and the time-integrated flux density ϕ_b was automatically determined. The electron flux density was also measured, before and after each irradiation, on a sliding Faraday cup located in front of the samples, and lowered to stop the electron beam during the resistivity measurements. The integrated flux ϕ_f on the sliding Faraday cup was determined from the value of ϕ_b and from the ratio between the electron flux densities on the Faraday cup behind the samples and on the sliding cup, i_b and i_f, respectively:

$$\phi_f = (i_f/i_b)\phi_b. \quad (1)$$

Because of the dispersion of the electrons in the steel window and in the hydrogen bath, the actual flux on the samples, ϕ_s, is intermediate between ϕ_f and ϕ_b. To obtain ϕ_s, the values of ϕ_f were corrected by reference to experimental calibrations performed by Gosset et al. in the same irradiation device [8,9].

3. Corrections of the experimental data

Before analyzing and fitting the experimental data with theoretical models, some corrections are required: the electrons coming from the accelerator, which initially form a parallel and monoenergetic beam, are slowed down and scattered by passing through different materials (25 μm thick steel window, 1.5 mm liquid hydrogen and within the samples themselves). Therefore, the measured values of energy and of fluence must be corrected.

3.1. Electron energy losses

The energy losses in the window and in the liquid hydrogen bath were both estimated from the determinations given by Gosset [8,9]. The energy losses in the samples themselves were deduced from the tabulations of Pages et al. [21] calculated for all the chemical elements. In TiAl, the energy losses were evaluated by including the weighted corrections related to the composition of the compound. The total correction was ~110 keV at 2.5 MeV for the $Ti_{50}Al_{50}$ alloy at half sample thickness.

3.2. Electron effective path corrections within the samples

Due to scattering, the effective path of electrons in the samples is larger than the thickness of the latter. Such an effect increases the probability of defect production and the experimental resistivity damage rates $(\Delta\rho/\Delta\phi)_{exp}$ were corrected by applying the theoretical expression proposed by Sherman [22] for electrons of constant energy:

$$(\Delta\rho/\Delta\phi)_{exp} = (1 + K \cdot e_m/\cos\theta)(\Delta\rho/\Delta\phi)_{corr}, \quad (2)$$

where K is a function of the electron energy and the density, atomic number and atomic mass of the material; θ is the incident angle of the electron beam (in our experimental conditions $\cos\theta \approx 1$). The electron energy used in the calculation of K was taken equal to the average energy, evaluated at half-sample thickness e_m. In TiAl, weighted values of density, atomic number and atomic mass of titanium and aluminium were calculated according to the composition of alloys. This correction leads to an important decrease of the resistivity damage rates with respect to the experimental values at the lowest electron energies (by ~50% at 0.4 MeV in $Ti_{50}Al_{50}$).

3.3. Corrected experimental data

The corrected experimental resistivity damage-rates in pure titanium and in TiAl alloys are given in Fig. 1 as a function of the electron energy evaluated half-way through the samples. The experimental points on the three curves present some scatter. This dispersion may be related to the uncertainty on the fluence received by

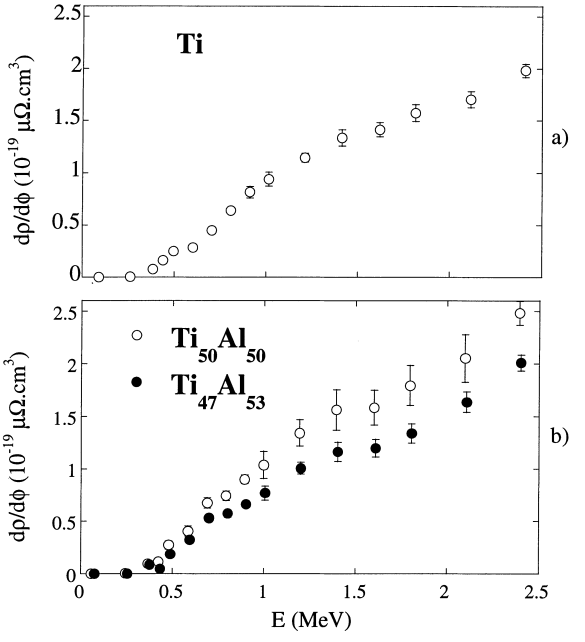

Fig. 1. Resistivity damage-rates as a function of electron energy (evaluated at half sample thickness) in polycrystalline (a) hcp-titanium; (b) $Ti_{50}Al_{50}$ and $Ti_{47}Al_{53}$.

the samples during irradiation. The resistivity damage rate curve for titanium shows that the minimum electron energy to produce permanent damage is ~0.275 MeV; a flat in the curve appears at ~0.5 MeV. In the TiAl compounds, it can be noted that the point at ~0.42 MeV is too low comparatively to the previous and next points. At this energy, the measured fluence is probably not correct. The two curves for the TiAl alloys have similar shapes, and the minimum electron threshold energy is around 0.3 MeV. However, the damage rates for the $Ti_{47}Al_{53}$ alloy appear to be lower at each energy than the ones of $Ti_{50}Al_{50}$.

4. Analysis of the experimental data

4.1. Relationships between resistivity damage rates and displacement cross-sections

In polycrystalline monoatomic metallic samples, the resistivity damage rates at different incident electron energies E are related to the displacement cross-sections for defect production σ_d:

$$(\Delta\rho/\Delta\phi) = p\rho_F\sigma_d(E, E_d), \tag{3}$$

where ρ_F is the Frenkel-pair resistivity per unit concentration, $p(0 < p \leqslant 1)$ is a defect production efficiency factor introduced to take into account the anisotropy effects on the displacement probabilities in polycrystalline samples (it characterizes the structural state of the polycristal), and E_d is the displacement threshold energy [8]. In this formalism, the value of $p\rho_F$ represents an effective Frenkel-pair resistivity. This relationship is valid when isolated Frenkel defects are produced, in the case of small fluences, and when the irradiation temperature is low enough to freeze point defect migration.

In polycrystalline diatomic alloys, the radiation damage is more complex than in monoatomic metals. The nature of the defects depends on the displacement cross sections of both types of atoms (in our case Ti and Al). For a low defect concentration, the resistivity damage rate can be written similarly to Eq. (3)

$$\Delta\rho/\Delta\phi = p^{Ti}\rho_F^{Ti}\sigma_d^{Ti}(E, E_d^{Ti}) + p^{Al}\rho_F^{Al}\sigma_d^{Al}(E, E_d^{Al}), \tag{4}$$

where σ_d^{Ti} and σ_d^{Al} are the respective displacement cross-sections of Ti and Al atoms, p_{Ti} and p_{Al} the correction coefficients for the displacement probabilities of Ti and Al atoms; ρ_F^{Ti} and ρ_F^{Al} are average values of the resistivity characterizing the different types of Frenkel-pairs which result from the displacement of Ti or Al atoms, respectively.

Moreover, the TiAl alloys are LRO materials. Thus, electron irradiation can produce both point defects and disordering, which both lead to a resistivity increase. Nevertheless, the disordering contribution to the resistivity damage rate, for irradiation by 2.5 MeV electrons, was estimated to be about 8% of the initial damage rate for the stoichiometric alloy, and even less for the high-Al TiAl alloys [11]. Therefore, the disordering contribution for TiAl alloys will be neglected in the evaluation of the displacement threshold energies.

4.2. Theoretical evaluations of the displacement cross-sections

To analyze the experimental data, resistivity damage rates should be compared to theoretical displacement cross-sections. For pure Ti, these were calculated up to 2.5 MeV electron energies by using Oen's tabulation [23] with threshold energies ranging from 20 to 30 eV. In the diatomic TiAl compound, the total displacement cross-section of a given type of atom is the sum of three terms related to:

1. the direct displacement of the atom by an electron (primary displacement); the minimum energy transfer necessary to obtain a stable defect is the so-called threshold displacement energy E_d;
2. the displacement of an atom via a collision cascade initiated by an atom of the same kind as the displaced atom;
3. the displacement of an atom via a collision cascade initiated by an atom of the other kind.

Analytical calculations of the number of displaced atoms and of the resulting displacement cross-sections have been performed by Lesueur for a polyatomic target [24]. This model is based on a single-step displacement function and on a single threshold energy for each atomic species. The restrictive hypotheses of this model are:

1. collisions are assumed to be elastic and the electronic energy losses of the primary atoms are neglected;
2. collision probabilities are assumed to be proportional to the atomic concentrations;
3. focusing or channelling effects and the crystal structure are not considered (the solid is amorphous-like).

The displacement cross-sections σ_d^{Ti} and σ_d^{Al} in TiAl were calculated up to electron energies of 2.5 MeV for a given threshold energy E_d^{Ti} (or E_d^{Al}) and different values of E_d^{Al} (or E_d^{Ti}) ranging from 20 to 38 eV, from the model proposed by Lesueur [24].

4.3. Methods used to analyze the experimental data

The displacement threshold energy in the irradiated materials was evaluated by two methods.

The first method (method 1) consists in comparing directly the experimental damage-rate curves to theoretical displacement cross-sections. The experimental resistivity damage rates are plotted as a function of the theoretical displacement cross-sections. For a pure metal, the correct value of E_d is the one which leads, according to Eq. (3), to a straight line passing through

the origin. The slope of the straight line gives the value of the effective Frenkel-pair resistivity $p\rho_F$.

In the case of diatomic compounds, some assumptions have to be made to use this method, since a direct fit of Eq. (4) is not possible due to the existence of four unknowns. Nevertheless, in the case of TiAl alloys, since aluminium is lighter than titanium, it is expected that aluminium displacement should be dominant at low electron energies. Fig. 2 shows the variations of theoretical displacement cross-sections for Al and Ti in TiAl with $E_d^{Ti} = 30$ eV and $E_d^{Al} = 33$ eV, as a function of incident electron energy, from Lesueur's calculation. On this particular example, the displacement cross-section of aluminium represents 100% of total cross-section between 0.3 and 0.45 MeV, and 75% at 0.5 MeV. From 0.65 MeV up, the displacement cross-section of titanium becomes larger than the one of aluminium. Therefore, aluminium displacement predominantly influences the curves in the low energies range, and the value of the minimum electron energy required to observe a beginning of resistivity variations is only sensitive to E_d^{Al}. At higher energies, the shape of the curves is more influenced by titanium displacement and so it depends mainly on E_d^{Ti}.

Consequently, we can suppose that only Al atoms are displaced in the energy range 0.3–0.5 MeV. Then, relationship (4) becomes

$$(\Delta\rho/\Delta\phi) = p^{Al}\rho_F^{Al}\sigma_d^{Al}(E, E_d^{Al}) \quad \text{for } 0.3 \text{ MeV} \leqslant E \leqslant 0.5 \text{ MeV}. \tag{5}$$

The linear fitting of experimental data $\Delta\rho/\Delta\phi$ to calculated values σ_d^{Al} allows one to obtain E_d^{Al} and the effective Frenkel-pair resistivity $P_{Al}\rho_F^{Al}$. When electron energy becomes larger than about 0.5 MeV, Ti atoms are also displaced. The increase of damage rate with incident electron energy E is given by the general relationship (4),

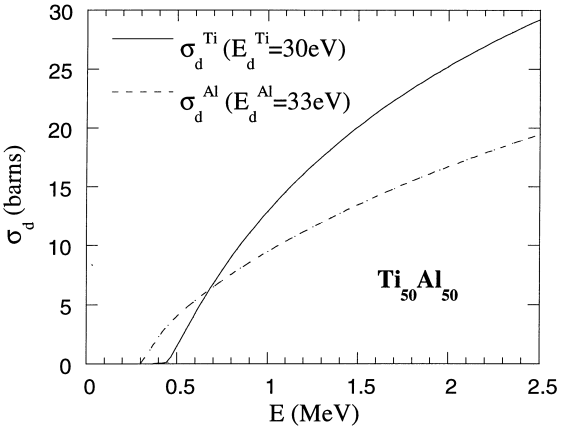

Fig. 2. Theoretical displacement cross-sections of Ti (with $E_d^{Ti} = 30$ eV) and Al (with $E_d^{Al} = 33$ eV) as a function of incident electron energy in $Ti_{50}Al_{50}$ alloy.

in which the term $p^{Al}\rho_F^{Al}\sigma_d^{Al}(E, E_d^{Al})$ can now be calculated for all values of E. The contribution of Frenkel-pairs, due to Ti displacement, to the total increase of resistivity can be written as

$$(\Delta\rho/\Delta\phi)^{Ti} = p^{Ti}\rho_F^{Ti}\sigma_d^{Ti}(E, E_d^{Ti}) = (\Delta\rho/\Delta\phi)^{exp} - p^{Al}\rho_F^{Al}\sigma_d^{Al}(E, E_d^{Al}). \tag{6}$$

The values E_d^{Ti} and $P_{Ti}\rho_F^{Ti}$ can be derived also by a linear fitting of $(\Delta\rho/\Delta\phi)^{Ti}$ versus σ_d^{Ti} in the 0.4–1.2 MeV range. With this procedure, both effective Frenkel-pair resistivities for Ti or Al can be determined.

In the second method (method 2), the experimental resistivity damage rates and the theoretical displacement cross-sections are normalized to values corresponding to an arbitrarily chosen reference electron energy (here 1.4 MeV). This relative method allows to reduce the number of unknowns for the determination of displacement threshold energies, with the assumption that the specific Frenkel-pair resistivities $p_{Ti}\rho_F^{Ti}$ and $p_{Al}\rho_F^{Al}$ are not very different. In this case, we can consider a unique effective value $p_{TiAl}\rho_F^{TiAl}$. With this approximation, Eq. (4) reduces to

$$\Delta\rho/\Delta\phi = p_{TiAl}\rho_F^{TiAl}\left(\sigma_d^{Ti}(E, E_d^{Ti}) + \sigma_d^{Al}(E, E_d^{Al})\right). \tag{7}$$

By normalizing the damage rates to a reference energy of 1.4 MeV for instance, we obtain

$$\frac{(\Delta\rho/\Delta\phi)_E}{(\Delta\rho/\Delta\phi)_{1.4}} = \frac{\sigma_d^{Ti}(E,\ E_d^{Ti}) + \sigma_d^{Al}(E,\ E_d^{Al})}{\sigma_d^{Ti}(1.4,\ E_d^{Ti}) + \sigma_d^{Al}(1.4,\ E_d^{Al})}. \tag{8}$$

In this case, the only adjustable parameters are the respective displacement threshold energies for Ti and Al. It may be noted that the same expression can be obtained if the disordering contribution is taken into account, with however some additional assumptions [5]. Like in method 1, the comparison of experimental data to theoretical curves consisted in, first, determining the E_d^{Al} value from an adjustment in the 0.3–0.5 MeV energy range, then fixing E_d^{Al} to the obtained value and adjusting E_d^{Ti}, to fit the results in the energy range 0.4–0.8 MeV.

5. Results and discussion

The experimental determination of displacement cross-sections requires that point defect concentrations introduced in the materials remain relatively low so that defects are isolated. This is the case in the present samples of pure Ti and TiAl compounds, since the resistivity damage-rates versus fluence were linear up to 2.5 MeV.

5.1. Pure hcp titanium

An attempt at applying method 1 to determine the threshold displacement energy of pure titanium, by fit-

ting the data in the whole energy range up to 2.5 MeV by a straight line, showed that systematic deviations occur: the high-energy data points are not aligned with the low-energy ones. Furthermore, a flat observed at 0.5 MeV on the damage-rate curve for Ti in Fig. 1(a) might suggest a change in the effective threshold energy above 0.5 MeV. If, nevertheless, the experimental data in the whole energy range are fitted with a single displacement energy, an average value of 26 ± 5 eV is obtained. Since the standard displacement cross-section model does not adequately represent high-energy processes (see the introduction of the efficiency factor, Eq. (3)), we distinguished two energy ranges for the analysis of the data: a first one from 0 to 0.5 MeV, which should yield the minimum threshold energy, and a second one from 0.5 to 2.5 MeV, which should correspond to an effective displacement energy over this range.

The fitting of experimental results by method 1, in the range 0–0.5 MeV, is shown in Fig. 3. The best fit is obtained with $E_d^{Ti} = 21 \pm 1$ eV. A value of 14.5 ± 2.0 μΩ cm/% can be determined for the effective Frenkel-pair resistivity $p\rho_F$. In the energy range 0.5–2.5 MeV, we obtained 30 ± 1 eV and 39 ± 2.0 μΩ cm/% for the titanium displacement energy and for the effective Frenkel-pair resistivity, respectively.

To apply method 2, the normalized experimental displacement cross-sections (points in Fig. 4) were plotted as a function of electron energy midway through the polycrystalline titanium sample (E) together with the theoretical curves (lines) calculated for threshold energies ranging from 20 to 30 eV. The comparison of the data leads to the conclusion that the best fit is obtained with $E_d^{Ti} = 24 \pm 2$ eV for $E \leqslant 0.5$ MeV, and with $E_d^{Ti} = 30 \pm 2$ eV for the higher electron energies.

The present results are in agreement with the previously published data if the comparison is made in the corresponding electron energy ranges. In the low energy range (0.3–0.5 MeV), the results of Shirley and Chaplin [17] and the present data are presented in Fig. 5, showing the evolution of resistivity damage rates as a function of the maximum atomic recoil energy E_M, related to electron energy E by

$$E_M = 2E(E + 2mc^2)/Mc^2, \tag{9}$$

where c is the speed of light, m the mass of the electron and M the mass of the recoil atom. The similarity of the results between these two investigations is reflected in the threshold energy values: 19.2 ± 1.0 eV for Shirley and Chaplin and 21 ± 1 eV (by method 1) in the present work; the corresponding effective Frenkel-pair resistivities $p\rho_F$ were also very similar (14–18 μm cm/% for Shirley and Chaplin and 14.5 μm cm/% for our experiments in the same energy range). Moreover, a value of 22.3 ± 0.3 eV, close to the present results, was derived from experiments of radiation damage in a high voltage electron microscope operated at voltages up to 410 kV [25].

On the other hand, from experiments performed in the electron energy range 0.5–1.4 MeV, Lucasson and Walker [16] have determined a displacement threshold energy in Ti equal to 29 eV and a value of 42 μm cm/% for the Frenkel-pair resistivity, close to our results in the same range. Therefore, for higher electron energies, it

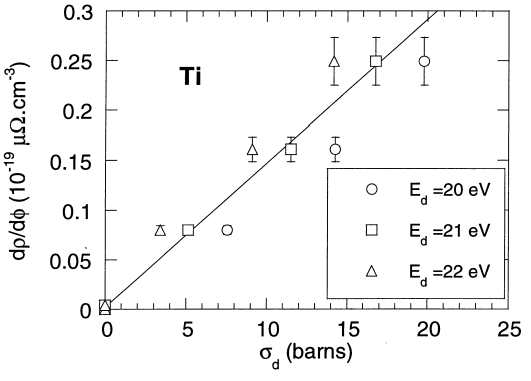

Fig. 3. Evolution of resistivity damage rate ($\Delta\rho/\Delta\phi$) as a function of theoretical displacement cross-sections σ_d for different threshold energies (20, 21 and 22 eV) in hcp titanium, in the electron energy range 0.3–0.5 MeV.

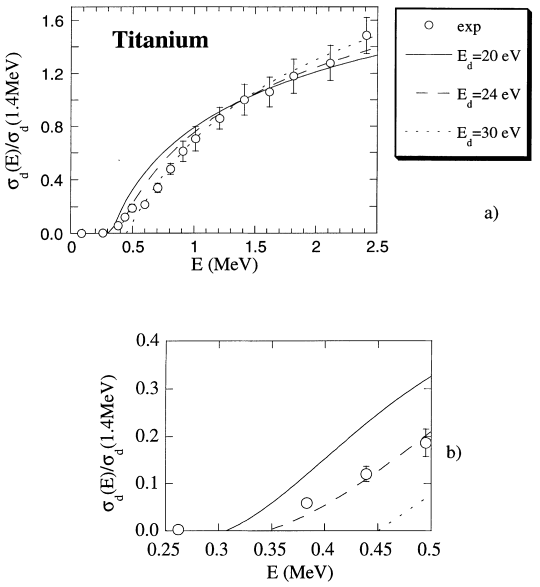

Fig. 4. Experimental normalized displacement cross-section as a function of electron energy (midway through the sample) in polycrystalline titanium (points) and theoretical variations (lines) calculated with threshold energies $E_d^{Ti} = 20$, 24 and 30 eV (a) in the whole energy range; (b) in the energy range 0.25–0.5 MeV.

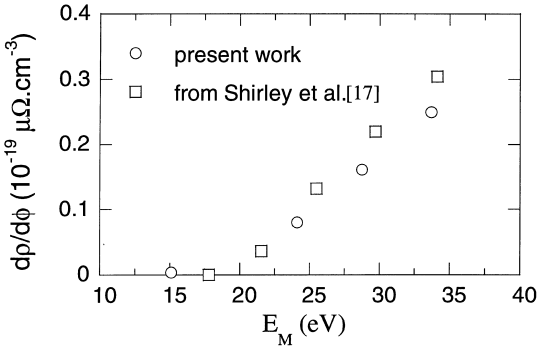

Fig. 5. Evolution of resistivity damage rate ($\Delta\rho/\Delta\phi$) as a function of the maximum atomic recoil energy E_M in pure titanium, from Shirley et al. [17] and present results.

appears that the effective displacement energy in Ti is higher (~30 eV) than when $E \leqslant 0.5$ MeV.

The titanium used in the present work had a very high purity. Nevertheless, our results are very close to the ones obtained in the other investigations, in which the purity of Ti was certainly not the same. Therefore, the two displacement energy values obtained according to the energy range should not be related to displacements of impurity atoms occurring below the threshold. On the other hand, these differences might originate from the orientation dependence of the threshold displacement energy. At low electron energies, the experiments will yield the minimum value of this parameter, whereas the analysis of higher-energy experiments will be described by an effective displacement energy, resulting from an average over soft and hard orientations. This effect has been documented in other hcp metals, like Zn and Cd [25].

The existence of orientation effects in α-Ti is supported by a computer simulation study of displacement cascades by molecular dynamics [26,27]. A strong dependence on orientation of the displacement threshold energy was found, ranging from minima of 12.5 eV for orientations near [$\bar{2}$ 2 0 1] to 57.5 eV for several directions between [0 0 0 1] and [$\bar{1}$ 2 $\bar{1}$ 0]. However, the mean value of E_d found by integration over the 33 orientations chosen for the simulations was approximately 30 eV [27], which is comparable to the effective displacement energy found in the present work, in the higher electron energy range.

5.2. TiAl alloys

The fitting of experimental results in the stoichiometric compound by method 1, as discussed in Section 4.3, is shown in Fig. 6(a) and (b). Figs. 7 and 8 compare (method 2) in $Ti_{50}Al_{50}$ the normalized displacement cross-sections, experimentally determined as

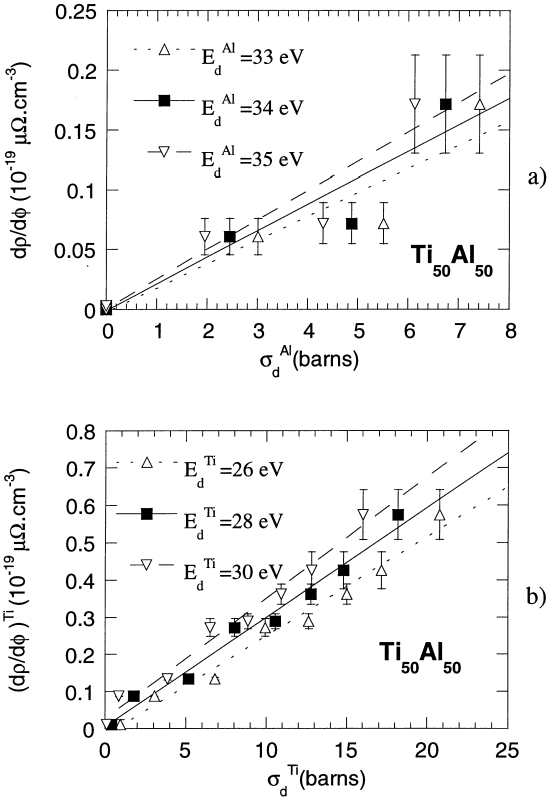

Fig. 6. (a) Evolution of resistivity damage rate ($\Delta\rho/\Delta\phi$) as a function of theoretical Al displacement cross-sections σ_d^{Al} for different aluminium threshold energies ($E_d^{Al} = 33$, 34 and 35 eV), in the incident electron energy range 0.3–0.5 MeV; (b) evolution of resistivity damage rate related to Ti displacement $(\Delta\rho/\Delta\phi)^{Ti}$ as a function of theoretical Ti displacement cross-sections σ_d^{Ti} for different Ti threshold energies ($E_d^{Ti} = 26$, 28 and 30 eV), in the incident electron energy range 0.4–1.2 MeV, in $Ti_{50}Al_{50}$.

a function of the electron energy E, with theoretical curves calculated in the model proposed by Lesueur [24] with a constant E_d^{Ti} (or E_d^{Al}) threshold energy and E_d^{Al}(or E_d^{Ti}) values varying in steps of 2 eV. In both methods, the fitting procedure consists in first determining the E_d^{Al} value in the low energies range for a constant E_d^{Ti}, then fixing E_d^{Al} to the obtained value and adjusting E_d^{Ti}. Similar results were obtained in $Ti_{47}Al_{53}$. The displacement threshold energies of Ti and Al resulting from the best fit of the experiments and the effective Frenkel-pair resistivity $p_{TiAl}\rho_F^{TiAl}$ calculated at 1.5 MeV are given in Table 2 for the $Ti_{50}Al_{50}$ and $Ti_{47}Al_{53}$ alloys. The values of E_d^{Ti}, E_d^{Al} and of the specific Frenkel-pair resistivities $p_{Ti}\rho_F^{Ti}$ and $p_{Al}\rho_F^{Al}$ determined by method 1 are also reported.

It can be seen that the effective Frenkel-pair resistivities related to the displacement of Ti or Al atom, obtained by method 1, are not too different. This result validates the assumption of method 2 for which a unique

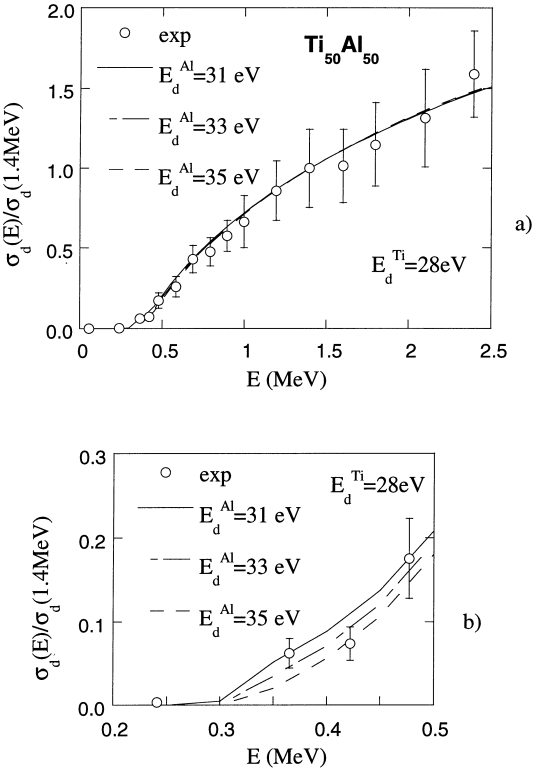

Fig. 7. Experimental normalized displacement cross-section as a function of electron energy (midway through the sample) in the $Ti_{50}Al_{50}$ alloy (points) and theoretical variations (lines) calculated with threshold energies $E_d^{Ti} = 28$ eV and $E_d^{Ti} = 31$–35 eV (a) in the whole energy range; (b) in the energy range 0.2–0.5 MeV.

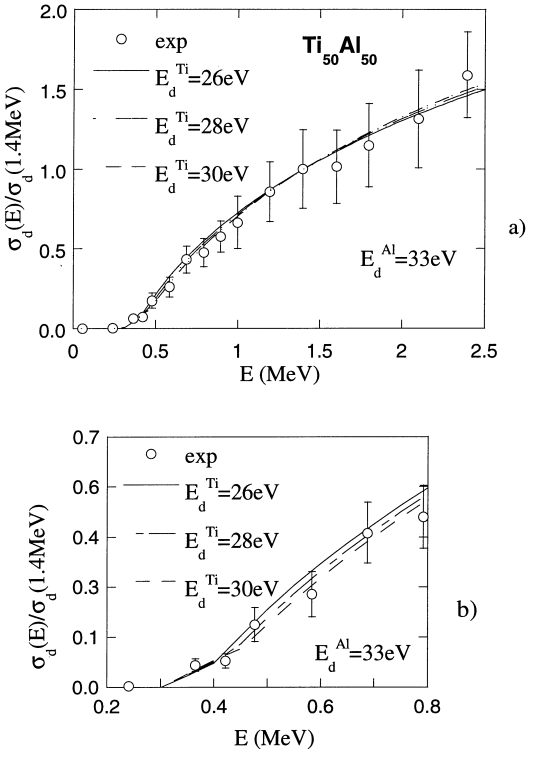

Fig. 8. Same as Fig. 7 with $E_d^{Al} = 33$ eV and $E_d^{Ti} = 26$–30 eV (a) in the whole energy range; (b) in the energy range 0.2–0.5 MeV.

value $p_{TiAl}\rho_F^{TiAl} \approx p_{Ti}\rho_F^{Ti} \approx p_{Al}\rho_F^{Al}$ was taken. The displacement threshold energies derived from the two methods are similar. Considering the uncertainties on the obtained values, no significant effect of alloy composition on threshold energies and effective Frenkel-pair resistivities is observed. Whatever the method applied, the threshold displacement energy E_d^{Al} of Al in TiAl ($\sim$34 eV) is much higher than the one in pure aluminium (16 eV [28]); it also appears to be somewhat higher than E_d^{Ti} in TiAl ($\sim$28 eV). In the intermetallic compound Ni_3Al, the displacement threshold energy of Al was also found larger (30 ± 2 eV) than the one of Ni (24 ± 1 eV) [5]. The displacement energy E_d^{Ti} of Ti in TiAl ($\sim$28 eV) entails more uncertainty since it is necessarily determined in an energy range farther from the threshold energy. However, it appears to be close to the value obtained in pure Ti for the higher energy range ($\sim$30 eV), in the present experiments.

The high displacement threshold energy for aluminium in TiAl could be related to the strong cohesion between Ti and Al (0 0 1) planes found by electronic structure calculations [29,30]. The case of Ti atoms is not so clear. A similar assumption was made by Gosset et al. to explain the stronger value of the displacement threshold energy of tantalum in TaC, the structure of which involves very strong covalent bonds, comparatively to Ta metal [8,9].

Recently, molecular dynamics simulations using N-body potentials were performed for calculating displacement threshold energies of Ti and Al in TiAl [15]. In most directions, the displacement threshold energies for aluminium primary knock-on atoms (PKA) were found to be larger than those for Ti PKA, except in [1 1 0] and [1 0 0] directions. The easiest directions of displacement were [1 1 0] (with $E_d^{Al} = 16$ eV and $E_d^{Ti} = 20$ eV), [1 0 0] ($E_d^{Al} = 18$ eV and $E_d^{Ti} = 19$ eV), [1 0 1] ($E_d^{Al} = 20$ eV and $E_d^{Ti} = 17$ eV) and [0 0 1] $E_d^{Al} = 27$ eV and $E_d^{Ti} = 26$ eV). Thus, in most cases, the results of Wang et al, showing that displacement threshold energy for Al is larger than for Ti in TiAl, are in agreement with our experimental data.

5.3. Evaluation of the Frenkel-pair resistivity in γ-TiAl

The Frenkel-pair resistivity ρ_F of γ-TiAl alloys with aluminium contents in the range 50–54 at.% Al have been previously estimated by a relative method, in which

Table 2
Displacement threshold energy of titanium and aluminium, and effective Frenkel-pair resistivity determined by two methods (see text), in $Ti_{50}Al_{50}$ and $Ti_{47}Al_{53}$ alloys

Alloy		$Ti_{50}Al_{50}$	$Ti_{47}Al_{53}$
Method 1			
($0.3 \leqslant E \leqslant 0.5$ MeV)	E_d^{Al} (eV)	34 ± 2	36 ± 2
	$p_{Al}\rho_F^{Al}$ (μΩ cm/%)	22 ± 3	20 ± 3
($0.4 \leqslant E \leqslant 1.2$ MeV)	E_d^{Ti} (eV)	28 ± 2	30 ± 2
	$p_{Ti}\rho_F^{Ti}$ (μΩ cm/%)	30 ± 3	29 ± 4
Method 2			
($0.3 \leqslant E \leqslant 0.5$ MeV)	E_d^{Al} (eV)	33 ± 2	35 ± 2
($0.4 \leqslant E \leqslant 0.8$ MeV)	E_d^{Ti} (eV)	29 ± 3	30 ± 3
	$p_{TiAl}\rho_F^{TiAl}$ (at 1.5 MeV) (μΩ cm/%)	29 ± 3	24 ± 3

the initial resistivity damage-rates of the investigated alloys were compared to the one of a simultaneously irradiated nickel sample [11]

$$\rho_F^{TiAl} = \left[p_{Ni}\sigma_d^{Ni}/p_{TiAl}\sigma_d^{TiAl}\right]\left[\dot{\rho}_0^{TiAl}/\dot{\rho}_0^{Ni}\right]\rho_F^{Ni}, \quad (10)$$

where ρ_F^{TiAl} and ρ_F^{Ni} are the respective Frenkel-pair resistivities of the nickel and of the $Ti_{50}Al_{50}$ alloy, $\dot{\rho}_0^{Ti_{50}Al_{50}}$ and $\dot{\rho}_0^{Ni}$ are the initial resistivity damage rates for the $Ti_{50}Al_{50}$ and the nickel respectively, $\sigma_d^{Ti_{50}Al_{50}}$ and σ_d^{Ni} are the displacement cross-sections for the $Ti_{50}Al_{50}$ and the nickel. This relative method allowed one to reduce the effect of the uncertainties in the absolute values of the electron flux and of the displacement cross-sections. However, the results involved two assumptions which could be criticized:

(i) the magnitude of the defect production efficiencies p (which can be considered as a measure of the deviation of the experimental cross-sections from theoretical values calculated in the case of a one-step displacement model, and is related to the crystal structure of the irradiated material) was assumed to be the same in fcc nickel and in the alloys, since TiAl is tetragonal with a c/a ratio close to 1; its structure can thus be considered as pseudo-fcc.

(ii) for the evaluation of the displacement cross-sections of Ti and Al in TiAl, threshold displacement energies determined in the pure metals were used.

With the displacement threshold energies obtained in the present experiments, it is possible to determine the Frenkel-pair resistivity of stoichiometric TiAl from the $p_{TiAl}\rho_F^{TiAl}$ value (Table 2), and also to reevaluate the previously published data [11], provided the value of p is known.

For a number of fcc metals (aluminium, copper and nickel), systematic deviations, i.e. $p \neq 1$, are observed between the theoretical and the experimental displacement cross-sections. For example, in nickel, an effective Frenkel-pair resistivity $p\rho_F$ of 1.91 ± 0.14 μΩ cm/% at 1.5 MeV was determined [31]. From this result, together with the Frenkel-pair resistivity of nickel (6.7 ± 0.4 μΩ cm/% [32]), a value of $p = 0.29 \pm 0.04$ is obtained. From 1.5 MeV electron irradiation data [28,31,33], p values are obtained in the range 0.22–0.44. Thus, we shall assume $0.22 < p^{TiAl} < 0.44$ at 1.5 MeV. From the effective Frenkel pair resistivity $p_{TiAl}\rho_F^{TiAl}$ given in Table 2 and taking into account a disordering contribution of ~8% (estimated in [11]) to the resistivity increase under irradiation, we obtained $\rho_F^{TiAl} = 99 \pm 33$ μΩ cm/%.

With the present displacement energies of Ti and Al in TiAl, a reevaluation of the Frenkel-pair resistivity previously obtained in Ref. [11] was performed. The p values at 2.5 MeV for cfc metals range from 0.17 to 0.39 (0.24 for nickel). Taking into account the disordering contribution (~8%) to the resistivity increase [11] and with the data reported in Table 3, a Frenkel-pair resistivity of 108 ± 42 μΩ cm/% for the stoichiometric TiAl alloy is obtained, which is close to the determined value as above from the present effective Frenkel-pair resistivity.

Although the set of the possible values for the Frenkel-pair resistivity of the stoichiometric TiAl alloy is relatively wide, these values are much larger than the Frenkel-pair resistivity of the pure metals (4.2 μΩ cm/% for example in Al [34]). They are of the same order of magnitude as the value determined for the stoichiometric Ni_3Al intermetallic compound (102 μΩ cm/%) [35].

6. Conclusion

In order to determine experimental threshold energy values for the displacement of titanium and aluminium in long-range ordered TiAl compounds and of Ti in hcp titanium, resistivity damage rates were measured during 21 K irradiations with electrons in the energy range 0.3–2.5 MeV. Displacement cross-sections derived from the variations of resistivity damage rates were compared

Table 3
Displacement threshold energies (E_d), relative displacement cross-section and initial damage rates resulting from defect contribution ($\dot{\rho}_0^{def}$) after irradiation with 2.5 MeV electrons [11], for nickel and the stoichiometric TiAl compound

Materials	Ni	$Ti_{50}Al_{50}$	
		Ti	Al
E_d (eV)	23 ± 1 [5]	29 ± 2	33 ± 3
$\sigma_d^{Ni}/\sigma_d^{TiAl}$	–	2.084	2.084
$\dot{\rho}_0^{def}$ (10^{-25} Ω cm^3)	0.234 ± 0.001 [11]	1.80 ± 0.07 [11]	1.80 ± 0.07 [11]

with theoretical curves determined in a single step displacement model for atomic species in polyatomic materials, as a function of electron energy. From the adjustment of the experimental data with calculated displacement cross-sections, the following results were obtained:

1. the displacement energy in hcp titanium is equal to 21 ± 1 eV in the energy range 0.3–0.5 MeV, and to 30 ± 2 eV in the energy range 0.5–2.5 MeV;
2. the displacement threshold energy of aluminium in the $Ti_{50}Al_{50}$ alloy is $E_d^{Al} = 34 \pm 2$ eV, much larger than the one found in pure aluminium and also somewhat higher than the displacement energy of titanium $E_d^{Ti} = 28 \pm 2$ eV in this intermetallic compound;
3. the displacement threshold energy of titanium in TiAl is about the same as the one found in hcp titanium in the energy range 0.5–2.5 MeV;
4. the Frenkel-pair resistivity of the stoichiometric TiAl compound was reevaluated from the displacement threshold energies of Ti and Al atoms determined in the present work. A value of the order of 104 μΩ cm/% was obtained.

Acknowledgements

The authors are grateful to Dr J. Bigot (CECM, Vitry) for providing the high-purity titanium, to Dr C. Dimitrov (CECM, Vitry) for her participation in the sample preparation and in the irradiation experiments, and to J. Ardonceau and S. Guillous (LSI-CEA-Ecole Polytechnique, Palaiseau) for their help during electron irradiations.

References

[1] S. Mori, H. Miura, S. Yamazaki, T. Suzuki, A. Shimizu, Y. Seki, T. Kunugi, S. Nishio, N. Fujisawa, A. Hishinuma, M. Kikuchi, Fusion Tech. 21 (1992) 1744.
[2] K. A Hishinuma, K. Nakata, K. Fukai, K. Ameyama, M. Tokizane, J. Nucl. Mater. 199 (1993) 167.
[3] A. Hishinuma, J. Nucl. Mater. 239 (1996) 267.
[4] A. Hishinuma, M. Tabuchi, T. Sawai, K. Nakata, Phys. Stat. Sol. (a) 167 (1998) 521.
[5] C. Dimitrov, B. Sitaud, O. Dimitrov, J. Nucl. Mater. 208 (1994) 53.
[6] A. Alamo, C.H. de Novion, D. Lesueur, M. Dirand, Radiat. Eff. 70 (1983) 157.
[7] A. Alamo, C.H. de Novion, G. Desarmot, Radiat. Eff. 88 (1986) 69.
[8] D. Gosset, Rapport CEA R-5381, 1987.
[9] D. Gosset, J. Morillo, C. Allison, C.H. de Novion, Radiat. Eff. Def. Solids 118 (1991) 207.
[10] F. Rullier-Albenque, J.P. Sénateur, Radiat. Eff. 88 (1986) 17.
[11] G. Sattonnay, F. Ma, C. Dimitrov, O. Dimitrov, J. Phys.: Condens. Matter 9 (1997) 5527.
[12] Y. Shirai, M. Yamaguchi, Mater. Sci. Eng. A 152 (1992) 173.
[13] R. Würschum, K. Badura-Gergen, E.-A. Kümmerle, C. Grupp, H.-E. Schaefer, Phys. Rev. B 54 (1996) 849.
[14] G. Sattonnay, C. Dimitrov, C. Corbel, O. Dimitrov, Intermetallics 7 (1999) 23.
[15] B.-Y. Wang, Y.-X. Wang, Q. Gu, T.-M. Wang, Comput. Mater. Sci. 8 (1997) 267.
[16] P.G. Lucasson, R.M. Walker, Phys. Rev. 127 (1962) 485.
[17] C.G. Shirley, R.L. Chaplin, Phys. Rev. B 5 (1972) 2027.
[18] C. Dimitrov, J.-L. Pastol, J. Bigot, O. Dimitrov, J. Phys. (Paris) IV, Colloque C7, 4 (1993) 481.
[19] G. Sattonnay, thesis, University Paris XI, 1998; Acta Mater. 47 (1999) in press.
[20] P. Lehr, in: G. Chaudron (Ed.), Monographies sur les métaux de haute pureté (tome II), Masson, Paris, 1977, p. 184.
[21] L.H. Pages, E. Bertel, H. Joffre, L. Sklavenitis, Rapport CEA R-3942, 1970.
[22] C.H. Sherman, Park. Mathem. Labs report No. 2, Contract AF19(628) 2419, 1963.
[23] O.S. Oen, Report ORNL 4897, 1973.
[24] D. Lesueur, Philos. Mag. A 44 (1981) 905.
[25] A.S.A. Karim, M.E. Whitehead, M.H. Loretto, R.E. Smallman, Acta Metall. 26 (1978) 975.
[26] D.J. Bacon, A.F. Calder, J.M. Harder, S.J. Wooding, J. Nucl. Mater. 205 (1993) 52.
[27] S.J. Wooding, D.J. Bacon, W.J. Phythian, Philos. Mag. A 72 (1995) 1261.
[28] B.W. Iseler, H.I. Dawson, A.S. Mehner, J.W. Kauffman, Phys. Rev. 146 (1966) 468.
[29] C.L. Fu, M.H. Yoo, Intermetallics 1 (1993) 59.
[30] Y. Song, S.P. Tang, J.H. Xu, O.N. Mryasov, A.J. Freeman, Philos. Mag. B 70 (1994) 987.
[31] B. Sitaud, thesis, University Paris VI, 1991.

[32] C. Dimitrov, O. Dimitrov, Radiat. Eff. 84 (1985) 117.
[33] H.J. Wollenberger, in: A. Seeger, D. Schumacher, W. Schilling, J. Diehl (Eds.), Vacancies and Interstitials in Metals, North Holland, Amsterdam, 1969, p. 215.
[34] P. Ehrhart, H.G. Haubold, W. Schilling, Adv. Solid State Phys. 14 (1974) 87.
[35] C. Dimitrov, B. Sitaud, X. Zhang, O. Dimitrov, U. Dedek, F. Dworschak, J. Phys.: Condens. Matter 4 (1992) 10199.